BIOCHEMISTRY
including biophysical chemistry & molecular biology

Article

pubs.acs.org/biochemistry

Complex Structures between the N-Type Calcium Channel ($Ca_V2.2$) and ω-Conotoxin GVIA Predicted via Molecular Dynamics

Rong Chen* and Shin-Ho Chung

Research School of Biology, Australian National University, Canberra, ACT 0200, Australia

Supporting Information

ABSTRACT: The N-type voltage-gated Ca^{2+} channel $Ca_V2.2$ is one of the important targets for pain management. ω-Conotoxins isolated from venoms of cone snails, which specifically inhibit $Ca_V2.2$, are promising scaffolds for novel analgesics. The inhibitory action of ω-conotoxins on $Ca_V2.2$ has been examined experimentally, but the modes of binding of the toxins to this and other related subfamilies of Ca^{2+} channels are not understood in detail. Here molecular dynamics simulations are used to construct models of ω-conotoxin GVIA in complex with a homology model of the pore domain of $Ca_V2.2$. Three different binding modes in which the side chain of Lys2, Arg17, or Lys24 from the toxin protrudes into the selectivity filter of $Ca_V2.2$ are considered. In all the modes, the toxin forms a salt bridge with an aspartate residue of subunit II just above the EEEE ring of the selectivity filter. Using the umbrella sampling technique and potential of mean force calculations, the half-maximal inhibitory concentration (IC_{50}) values are calculated to be 1.5 and 0.7 nM for the modes in which Lys2 and Arg17 occlude the ion conduction pathway, respectively. Both IC_{50} values compare favorably with the values of 0.04−1.0 nM determined experimentally. The similar IC_{50} values calculated for the different binding modes demonstrate that GVIA can inhibit $Ca_V2.2$ with alternative binding modes. Such a multiple-binding mode mechanism may be common for ω-conotoxins.

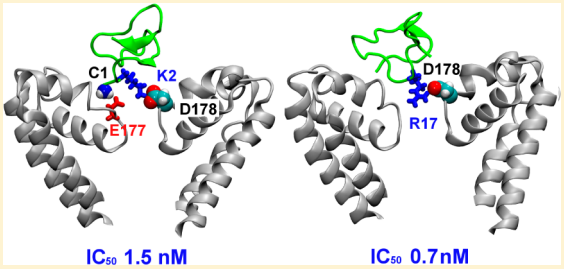

It has been estimated that 15−50% of adults suffer from chronic pain.[1] Several biological ion channels, including the N-type voltage-gated Ca^{2+} (Ca_V) channel Cav2.2, have been proposed as promising targets for the treatment of intractable pain. Ca_V channels are classified on the basis of gating and ion conduction properties into five subtypes, termed L, N, P/Q, R, and T types.[2] The ion conduction conduit of Ca_V channels is a large integral protein consisting of four homologous but nonidentical subunits (I−IV).[3] Each subunit comprises a voltage sensor, formed by four helices (S1−S4), and a pore domain formed by helices S5 and S6.[4]

Polypeptide toxins isolated from venoms of animals such as cone snails[5] and spiders[6] are promising molecular scaffolds from which novel analgesics targeting $Ca_V2.2$ may be developed.[7,8] For example, ω-conotoxin MVIIA, a selective blocker of $Ca_V2.2$, has been approved for the treatment of severe chronic neuropathic pain.[7,8] ω-Conotoxin CVID, another selective blocker of $Ca_V2.2$, is being subjected to extensive preclinical examination and clinical trials.[9] Development of peptide and nonpeptide mimetics of ω-conotoxins selectively targeting Cav2.2 is also being attempted.[5]

ω-Conotoxins block $Ca_V2.2$ via a pore blocking mechanism by physically occluding the ion conducting pathway.[10,11] The effect of ω-conotoxin GVIA on $Ca_V2.2$ can be inhibited by high concentrations of divalent ions such as Ba^{2+} and Ca^{2+} if the ions are applied before the toxin,[10,12,13] indicating that the toxin binds to the pore region of the channel. The mutation of neutral or acidic residues to positively charged basic residues on the outer vestibular wall of $Ca_V2.2$ reduces the blocking rate of the positively charged toxin GVIA appreciably,[11] consistent with a pore blocking mechanism.

ω-Conotoxins are short polypeptides consisting of 25−30 residues, whose backbones are interconnected by three disulfide bonds.[14] Available solution structures of ω-conotoxins show that they are typically globular in shape,[15] which makes them similar to μ-conotoxins that block voltage-gated Na^+ (Na_V) channels,[16−18] but the globular shape is different from the oval shape found in scorpion toxins that are potent blockers of voltage-gated K^+ (Kv) channels.[19] The shape of the toxins is important for their mechanism of action.[20] In the case of μ-conotoxin PIIIA, its six basic residues are approximately coplanar and symmetrically distributed. This allows the toxin to form similar interactions with the channel when different residues occlude the selectivity filter, and therefore, the toxin can block the channel with alternative binding modes with similar free energies.[17] In contrast, Kv channel blockers have a well-defined long principal axis, which is approximately perpendicular to the channel axis on block.[21] The modes of binding of ω-conotoxins to $Ca_V2.2$ are not understood in detail.

Here we construct a homology model of the pore domain of $Ca_V2.2$ and explore the modes of binding of GVIA to $Ca_V2.2$. GVIA is selected because it is one of the most extensively experimentally studied ω-conotoxins. The outer vestibule of

Received: March 14, 2013
Revised: April 29, 2013
Published: May 8, 2013

$Ca_V2.2$ is modeled on the crystal structure of the bacterial Na_V channel NavAb.[22] Three modes of binding of GVIA to $Ca_V2.2$ are predicted using a molecular docking method and molecular dynamics simulations. In these modes, Lys2, Arg17, and Lys24 of GVIA occlude the ion conduction pathway of $Ca_V2.2$. The IC_{50} values for two of the binding modes (Lys2 and Arg17) are calculated and compare favorably to those determined experimentally. It is found that the Lys2 mode and the Arg17 mode are equally favorable energetically. Such a multiple-binding mode mechanism may be common for ω-conotoxins, similar to that shown previously for the binding of μ-conotoxin PIIIA to NavAb.[17]

METHODS

Homology Model of $Ca_V2.2$. The crystal structures of the bacterial Na_V channel NavAb and several other similar bacterial Na_V channels have been reported.[22−25] The general architecture of Ca_V channels is similar to that of Na_V channels.[4] Thus, the available NavAb structure provides a template for homology modeling of human $Ca_V2.2$. However, because of the poor sequence similarity between bacterial and mammalian channels, the full sequence of $Ca_V2.2$ cannot be reliably modeled. Structurally, mammalian Ca_V and Na_V channels are hetero-tetramers and far more complex than homotetrameric bacterial channels. To model the pore domain of $Ca_V2.2$, we construct a chimera channel of $Ca_V2.2$ and NavAb. In this chimera, the outer vestibule of $Ca_V2.2$ is transferred to Na_VAb, as illustrated in Figure 1A.

The structure of the chimera channel is constructed by replacing the side chains of the residues in the outer vestibule of the NavAb structure with that of the corresponding residues from $Ca_V2.2$. The primary structures of the outer vestibule of NavAb and the four subunits of $Ca_V2.2$ are displayed in Figure 1B. It is seen that the selectivity filter residues are well aligned between the two channels. The four subunits (I−IV) of $Ca_V2.2$ are assembled clockwise according to available experimental evidence.[26,27]

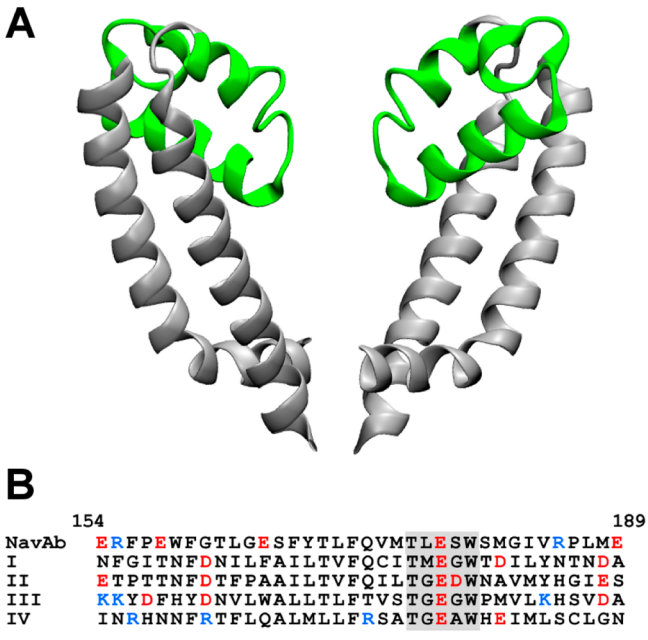

Figure 1. (A) Backbone of the $Ca_V2.2$−Na_VAb chimera with the $Ca_V2.2$ outer vestibule region colored green. Two subunits are shown for the sake of clarity. (B) Sequence alignment of $Ca_V2.2$ subunits I−IV and Na_VAb in the outer vestibule region. The five residues lining the selectivity filter are highlighted in gray. The numbering is that of Na_VAb.

Molecular Docking. To predict the position of GVIA relative to Cav2.2 on block, rigid-body docking program ZDOCK version 3.0.1[28] is used. Nuclear magnetic resonance (NMR) solution structure 2CCO[15] for GVIA is used. Channel residues that are not in the outer vestibule region are not expected to bind the toxin and therefore are not allowed to contact the toxin in the docking calculations. Each docking calculation generates 500 structures. A toxin residue is considered to occlude the filter if the distance between the centers of this residue and the EEEE ring of the channel filter (position 177) is less than 6 Å.

Molecular Dynamics (MD) Simulations. The $Ca_V2.2$ channel model is embedded in a POPC (2-oleoyl-1-palmitoyl-*sn*-glycero-3-phosphocholine) bilayer solvated with a rectangular box of explicit water, 0.1 M NaCl, and 0.1 M $CaCl_2$. The simulation box (90 Å × 90 Å × 110 Å) contains the channel protein, 162 lipids, 30 Na^+/Ca^{2+} ions, 91 Cl^- ions, and 15658 water molecules. The system is equilibrated for 10 ns. In the first 5 ns of the equilibration, harmonic restraint is applied to maintain a rigid channel backbone. The inner cavity of the channel is fully hydrated after the equilibration.

Toxin GVIA is then added to the system, with its center of mass (COM) 40 Å above the COM of the channel. At this distance, the toxin is not in direct contact with the channel. All Na^+ and Ca^{2+} ions except the Na^+ ion occupying the second binding site in the selectivity filter (see Figure 4) are removed from the system. This is to mimic the low ionic concentration used experimentally.[29] In addition, high concentrations of Ca^{2+} and Na^+ ions can inhibit GVIA binding.[13] The number of Cl^- ions is adjusted to maintain charge neutrality. To accelerate the binding of the toxin to the channel, flat-bottom harmonic distance restraints are applied to the side chain nitrogen atom of a basic residue of the toxin (Lys2, Arg17, or Lys24) and the center of the carbonyl groups of residue 177 in the selectivity filter of the channel. Similar methods have been used by Eriksson and Roux[30] and Chen and Chung[31] in the docking of voltage-gated K^+ (Kv) channel blockers. The upper boundary of the distance restraint is gradually decreased from 15 to 3 Å over a simulation period of 5 ns, such that the chosen basic residue of the toxin is drawn into the selectivity filter. The simulation is continued for an additional 25 ns with the harmonic restraints removed, allowing the system to evolve to a low-energy state.

MD simulations are performed at 1 atm and 300 K using NAMD version 2.9,[32] with periodic boundary conditions applied. The CHARMM36 force field and the TIP3P model for water are used to describe the interatomic interactions.[33−35] The switch and cutoff distances for short-range nonbonded interactions are 8.0 and 12.0 Å, respectively. The particle mesh Ewald method is used to account for long-range electrostatic interactions, with a maximal grid spacing of 1.0 Å. The SHAKE[36] and SETTLE[37] algorithms are used to keep the bond lengths in the system rigid. A time step of 2 fs is used. Trajectories are saved every 20 ps for analysis. Molecular graphics are generated using VMD.[38]

Umbrella Sampling. We derive with umbrella sampling the potential of mean force (PMF) profile for the unbinding of GVIA from $Ca_V2.2$ along the channel axis and calculate the half-maximal inhibition concentration (IC_{50}) of the toxin

dx.doi.org/10.1021/bi4003327 | *Biochemistry* 2013, 52, 3765−3772

block,[39,40] which can be observed experimentally. Previously using the same method, we predicted that PIIIA blocks Na_VAb with an IC_{50} of 30 pM,[17] only 6-fold larger than the value of 5 pM determined in subsequent experiments.[18] Thus, IC_{50} values of ion channel block by peptide toxins can be derived accurately from PMF calculations.

Steered molecular dynamics is applied to pull the toxin out from the binding site, allowing the starting structures of the umbrella windows spaced at 0.5 Å intervals to be generated. The backbones of both the toxin and the channel are kept rigid during the pulling. The COM of the toxin backbone is restrained to the center of each umbrella window using a harmonic force constant of 30 kcal mol^{-1} $Å^{-2}$. The COM of the channel is at z = 0 Å. A flat-bottom harmonic restraint is applied to maintain the COM of the toxin backbone within a cylinder with an 8 Å in radius centered on the channel axis. The radius of the cylinder is set to be sufficiently large that the restraining potential is always zero when the toxin is bound to the channel. This allows all the degrees of freedom of the toxin to be adequately sampled without bias. Each umbrella window is simulated for 5−8 ns until the depth of the PMF profile changes by <0.5 kT over the last 1 ns. The first 1 ns of each window is removed from data analysis. The z coordinate of the toxin COM is saved every 1 ps for analysis.

Data Analysis. A salt bridge is considered to be formed if the distance between a side chain oxygen atom from an acidic residue and a side chain nitrogen atom from a basic residue is less than 4 Å.[41] A hydrogen bond is considered to be formed if the donor and acceptor atoms (nitrogen or oxygen) are within 3.0 Å of each other and the donor−hydrogen−acceptor angle is ≥150°.[42] The weighted histogram analysis method is used to construct the PMF profile.[43] The IC_{50} value is derived using the following equation:[39,40]

$$IC_{50}^{-1} = 1000\pi R^2 N_A \int_{z_{min}}^{z_{max}} \exp[-W(z)/kT]\, dz \quad (1)$$

where R is the radius of the cylinder (8 Å), N_A is Avogadro's number, z_{min} and z_{max} are the boundaries of the binding site along the reaction coordinate (z), and $W(z)$ is the PMF. At the position where the toxin is fully bound to the channel, z = 24 Å, which defines the lower boundary of the binding site. The PMF is zero when z = 45 Å, which is the upper boundary of the binding site along z. We note here that eq 1 is valid only if appropriate flat-bottom cylindrical restraints are applied in deriving the PMF profile.[39,40]

RESULTS AND DISCUSSION

Structure of GVIA. Several mutagenesis experiments showed that the mutation of three basic residues (positions 2, 17, and 24) and two tyrosine residues (positions 13 and 22) each to alanine causes an appreciable reduction in the ability of the toxin to block $Ca_V2.2$.[44−46] Figure 2 shows that these five residues are spread over a large surface rather than clustered on one side of the toxin. In particular, the three basic residues, Lys2, Arg17, and Lys24, are approximately coplanar and symmetrically distributed on the surface of the toxin. Such symmetry resembles that of μ-conotoxin PIIIA, which blocks Na_VAb with alternative binding modes according to a recent computational study.[17] Thus, GVIA may also inhibit $Ca_V2.2$ via a multiple-binding mode mechanism, which we will demonstrate below.

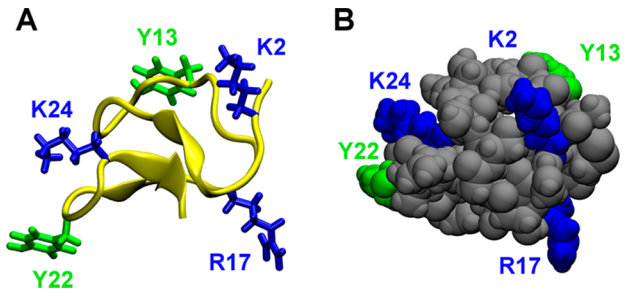

Figure 2. Molecular structure of GVIA with the side chains of five important residues highlighted. The primary structure of GVIA is CKSOG-SSCSO---> TSYNC-CRSCN-OYTKR-CY, where O indicates hydroxyproline. The C-terminus of GVIA is amidated. In panels A and B, the NewCartoon and VDW representations are used, respectively.

Outer Vestibule of $Ca_V2.2$. The homology model of $Ca_V2.2$, when equilibrated in a lipid bilayer and a box of water, reveals two rings of charged residues on the outer vestibule (Figure 3). The inner ring is formed by the EEEE motif of the selectivity filter, with the nearby Asp178 of subunit II and Arg172 of subunit IV, whereas the outer ring is formed by Asp188 of subunit I and Arg156 and Glu181 of subunit IV. These two rings of charged residues are separated by a ring of hydrophobic residues at position 182.

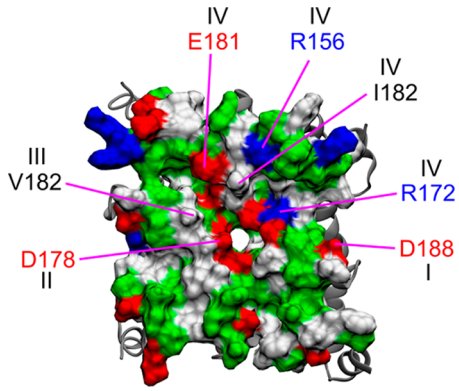

Figure 3. Outer vestibule of $Ca_V2.2$ viewed from the periplasmic side along the channel axis. Residues are colored as follows: basic, blue; acidic, red; polar, green; hydrophobic, white.

Glu181 and Asp188 of the outer ring are 13 and 17 Å from the central channel axis, respectively. Compared to the radii of 11−13 Å in the largest dimensions of GVIA, it appears that Glu181 but not Asp188 may be capable of forming a salt bridge with the toxin. However, the hydrophobic residues at position 182 whose side chains point toward the periplasmic side are located between Glu181 and the pore (Figure 3). The side chains of these hydrophobic residues may sterically prevent the toxin from binding Glu181 of subunit IV. This prediction is consistent with all the subsequent MD simulations described below. In none of these simulations was Glu181 observed to be in direct contact with the toxin.

Selectivity Filter of $Ca_V2.2$. The $Ca_V2.2$ channel contains two ion binding sites in the selectivity filter, which is evident from the equilibration simulation of 10 ns. The first binding site is at the entrance of the filter, formed by the side chains of the EEEE ring at position 177. Over a simulation period of 10 ns, a Na^+ ion binds to the first binding site at 3 ns. A Ca^{2+} ion is then attracted into the filter at 5 ns and knocks the Na^+ ion off to the

dx.doi.org/10.1021/bi4003327 | Biochemistry 2013, 52, 3765−3772

second binding site near the inner cavity of the channel. The two ions remain bound at the two sites over the remaining period of the simulation (Figure 4). The two ion binding sites

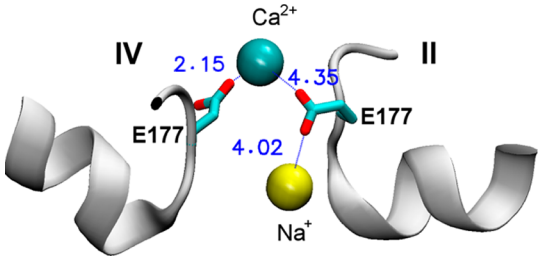

Figure 4. Two ions, one Ca^{2+} and one Na^{+}, bound to the selectivity filter of $Ca_V2.2$. The interatomic distances indicated are in angstroms.

of the $Ca_V2.2$ channel identified here are consistent with that of Na_VAb observed previously,[47] indicating that the model is able to reproduce important electrostatic interactions in the filter.

The overall structure of $Ca_V2.2$ appears to be reasonably stable. The maximal root-mean-square deviation of the channel backbone with respect to the initial model is 2.6 Å over the 10 ns simulation. The selectivity filter becomes narrower, from 5 to 2.5 Å in diameter, in the presence of the Ca^{2+} ion at the first binding site. This is because the Ca^{2+} ion attracts strongly the negatively charged side chains of Glu177 toward the center of the filter. In subsequent MD simulations, all Ca^{2+} ions are removed from the system as described in Methods. The diameter of the filter increases to ~4.5 Å when the side chain of a basic residue from the toxin protrudes into the filter.

Molecular Docking of GVIA. To explore the possible modes of binding between GVIA and $Ca_V2.2$, we use the rigid-body docking program ZDOCK[28] as described in Methods. Of the four basic residues at positions 2, 17, 24, and 25 of GVIA, only Arg17 is observed to occlude the selectivity filter in ~8% of the 500 structures generated. In all other structures, the filter is not blocked by the toxin. The docking calculation is repeated with a different structure of the toxin and the channel, and consistent results are observed. The predominant frequency of Arg17 occluding the filter observed in the docking calculations suggests that Arg17 of GVIA is the filter residue for $Ca_V2.2$ block. Mutagenesis experiments, however, suggest that Lys2 rather than Arg17 is the filter residue.[44,46]

The discrepancy between the docking calculations and mutagenesis experiment suggests that the toxin may block the channel with at least two binding modes, occluding the selectivity filter with the side chain of either Arg17 or Lys2. Such a multiple-binding mode mechanism has been demonstrated for μ-conotoxin PIIIA, which blocks Na_VAb potently with picomolar IC_{50} values.[17,18]

Modes of Binding of GVIA to $Ca_V2.2$. We reasoned that the side chains of several different basic residues in GVIA may be capable of protruding into the selectivity filter and interact with the acidic residues lining the filter. It is possible that the different binding modes are not revealed by the rigid-body docking program we used. To test this conjecture, we use biased MD simulations with distance restraints as a docking method.[30,31] This method allows any binding modes of interest to be examined, as distance restraints can be applied to arbitrary residue pairs between the toxin and the channel.

$Ca_V2.2$ is a heterotetramer, which renders docking using the biased MD simulation method challenging. For homotetrameric channels, sampling of interactions of toxins with only one channel subunit is needed. In contrast, the simulation must sample interactions of the toxin with all the four subunits of $Ca_V2.2$. This is not possible on a time scale of 30 ns. Rather, the system is likely to be trapped in a local minimal energy state and unable to cross the energy barrier to find the global minimal energy state. To circumvent the sampling problem, we repeat each biased MD simulation with a different starting configuration, in which the toxin is rotated by 180° along the z axis (see Figure S1 of the Supporting Information).

Figure 5A shows the structure of GVIA bound to the outer vestibule of $Ca_V2.2$ predicted from the biased MD simulation in

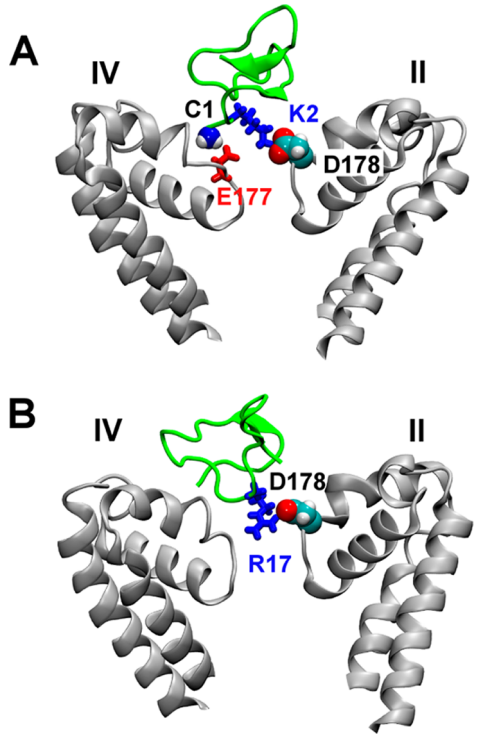

Figure 5. Positions of GVIA relative to the selectivity filter of $Ca_V2.2$ predicted from MD simulations with distance restraints. The toxin backbone is colored green.

which Lys2 of the toxin is selected as the filter residue. In this structure, Lys2 is observed to form strong electrostatic interactions with the selectivity filter and, in particular, residue Asp178 of subunit II by forming a salt bridge. The average length of this salt bridge over the last 5 ns of the simulation is 2.8 ± 0.2 Å, well below the cutoff distance of 4.0 Å for a salt bridge.[41] In addition to the Lys2−Asp178 salt bridge, a second strong interaction is observed between the protonated amine group of GVIA Cys1 and the carboxylate group of Glu177 of $Ca_V2.2$ subunit IV. A hydrogen bond is formed between GVIA Cys1 and $Ca_V2.2$ Glu177, with an average donor−acceptor distance of 3.0 ± 0.5 Å. No other salt bridges or hydrogen bonds are observed in the GVIA−$Ca_V2.2$ complex. Strong hydrophobic interactions are also observed between the toxin and the channel. In particular, Tyr13 of GVIA in addition to several other polar and nonpolar residues is found to be in the proximity of the four hydrophobic residues, including two valines and two isoleucines at position 182 of the channel. In the second simulation, the Lys2−Asp178 salt bridge but not the Cys1−Glu177 hydrogen bond is observed (Figure S2 of the

dx.doi.org/10.1021/bi4003327 | Biochemistry 2013, 52, 3765−3772

Supporting Information). This suggests that the final states predicted from the biased MD docking simulations could indeed be trapped in local energy minima. The first toxin−channel complex (Figure 5A) appears to be more energetically favorable and therefore is used in subsequent PMF calculations.

Figure 5B shows the structure of GVIA relative to the outer vestibule of $Ca_V2.2$ predicted from the biased MD simulation in which Arg17 is chosen as the filter residue. In this complex, Arg17 is observed to form a salt bridge with Asp178 of subunit II, similar to the Lys2−Asp178 salt bridge in the complex of Figure 5A. The average length of this salt bridge is 4.1 ± 0.3 Å, indicating a moderate coupling of Arg17 with Asp178. Arg17 is also found to form a salt bridge with Glu177 in the filter, with an average distance of 4.0 ± 0.3 Å. In addition, Tyr27 of GVIA is in close contact with the four hydrophobic residues at position 182 near the entrance of the filter. In the second simulation, the Arg17−Asp178 salt bridge is again observed (average length of 3.4 ± 0.1 Å). However, Arg17 penetrates slightly more shallowly into the filter (Figure S2 of the Supporting Information). The deep penetration of Arg17 observed in the first simulation may be energetically more favorable, and thus, the structure predicted from this simulation is used in subsequent PMF calculations.

PMF Profiles. To validate the models of GVIA bound to $Ca_V2.2$ predicted from biased MD simulations as shown in Figure 5, we construct the PMF profiles of toxin binding along the channel axis and derive the corresponding IC_{50} values. IC_{50} can be observed experimentally, providing a unique quantity on which the models could be verified.

The PMF profiles for the two binding modes in which Lys2 or Arg17 occludes the ion conduction pathway of $Ca_V2.2$ are shown in Figure 6. Figure S3 of the Supporting Information shows the convergence of the profiles. The two profiles virtually overlap for $z > 30$ Å, although they differ by ∼1 kT in the z range of 25−30 Å. The depth of the PMF profile for the Lys2 mode is only 0.7 kT shallower than that of the Arg17 mode, suggesting that these two binding modes are equally favorable. This is consistent with the interactions observed in the two binding modes (Figure 5). In the Lys2 mode, a hydrogen bond and a strong salt bridge between the toxin and the selectivity filter are formed, whereas in the Arg17 mode, two salt bridges of moderate strength are observed.

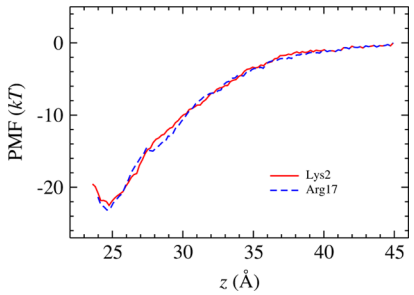

Figure 6. PMF profiles for the two binding modes in which Lys2 or Arg17 of GVIA occludes the ion conduction pathway of $Ca_V2.2$. The reaction coordinate z is the distance between the centers of mass of toxin and channel backbone atoms along the channel axis. The lower (z_{min}) and upper (z_{max}) boundaries of z are 24 and 45 Å, respectively.

The IC_{50} value of the Lys2 mode derived using eq 1 is 1.5 nM, only 2-fold higher than that of the Arg17 mode (0.7 nM). Experimentally, the IC_{50} value for the block of $Ca_V2.2$ by GVIA has been estimated to be 1 nM,[44] although values as low as 0.06 nM[48] and 0.04 nM[49] have been reported. The IC_{50} values derived for the Lys2 and Arg17 mode are in reasonable agreement with experiment. Thus, the PMF calculations indicate that the two binding modes are equally favorable energetically.

Interpretation of Available Experimental Results. Another way of validating the models is to compare them with mutagenesis data. However, such comparisons are often not straightforward. Several confounding factors must be considered in the interpretation of experimental results.[14] First, the backbone structure of the toxin may change after mutation. In fact, moderate to large conformational changes could be induced by mutation.[44,45] Second, the orientation of a toxin upon binding to a channel can be altered by mutation. The mutant toxin may bind with a different orientation such that the magnitude of the change in binding affinity is lower than expected. For example, if Lys2 of GVIA were the filter residue, mutating this residue to a charge-neutral one should significantly disrupt toxin−channel interactions. However, this is not seen experimentally,[45] as discussed in more detail below. Considering that direct comparison between our models and experiment is difficult, here we attempt to interpret the effect of Lys2 and Tyr13 mutations on the binding affinity of GVIA for $Ca_V2.2$ observed by Lew et al.[44] and Flinn et al.[45] in the context of our models.

The results of mutagenesis studies by Flinn et al.[45] are consistent with Lys2 being only one of the several possible filter residues. Among the five Lys2 mutants examined,[45] the K2A mutant causes the largest reduction (24−146-fold) in affinity. This large effect may be due to structural changes, as the chemical shift of the mutant toxin deviates significantly from that of the wild type.[44] The K2Nle mutant, which does not appear to induce significant conformational changes, reduces the binding affinity by 9−15-fold.[45] This corresponds to a free energy of 2−3 kT, which is ∼2 times lower than the free energy of 6−7 kT for a typical salt bridge in proteins.[50,51] We note that the filter residue not only forms a salt bridge with Asp178 of subunit II but also interacts favorably with the four glutamate residues at position 177. If the Lys2−Asp178 salt bridge were not replaced by an equivalent one, the binding affinity of GVIA would have been reduced by at least 300−1000-fold. Indeed, a similar mutation (K27Nle) of charybdotoxin reduces its affinity for Kv1.3 by 300-fold,[52] consistent with a unique filter residue mechanism. Therefore, both available evidence and our PMF calculations (Figure 6) are consistent with a multiple-filter residue mechanism for GVIA, similar to that observed for μ-conotoxin PIIIA.[17] To test whether Lys24 of GVIA is also a possible filter residue, two biased MD simulations with a distance restraint applied to Lys24 of GVIA and the filter of $Ca_V2.2$ are performed. It is found that the toxin binds tightly to the channel, with Lys24 forming a salt bridge with Asp178 of $Ca_V2.2$ subunit II similar to that observed in the Lys2 and Arg17 modes (Figure S4 of the Supporting Information). Therefore, the K27Nle mutant GVIA may use the side chain of either Arg17 or Lys24 to occlude the ion conduction pathway of $Ca_V2.2$ without a significant disruption of toxin−channel interactions.

The Tyr13 residue of GVIA may contribute to the binding primarily through entropic effects. The large change in affinity due to the Y13A mutation is at least partially due to conformational changes.[45] There are two types of interactions Tyr13 may form with the channel. The hydroxyl group of Tyr13 has the potential to form a hydrogen bond, whereas the

dx.doi.org/10.1021/bi4003327 | Biochemistry 2013, 52, 3765−3772

aromatic ring could form hydrophobic interactions. The free energy of a typical hydrogen bond in peptides is 1−3 kT in solution.[53,54] Therefore, the maximal change in affinity due to the Y13F mutation that does not disrupt the hydrophobic interactions should be 20-fold, in contrast to the larger changes of 110−470-fold observed experimentally,[45] suggesting that Tyr13 may be important for the structural integrity and rigidity of the toxin.

CONCLUSIONS

Here models of GVIA in complex with the outer vestibule of $Ca_V2.2$ are constructed using homology modeling and MD simulations. The models are validated against the IC_{50} values of toxin block determined experimentally and could well explain available mutagenesis data for the binding of GVIA to $Ca_V2.2$. Thus, our models provide the structural basis on which future experimental results may be interpreted.

The molecular docking program ZDOCK[17,21,55−57] and other docking algorithms[58,59] have been applied successfully to numerous toxin−channel systems. However, here the Lys2 and Lys24 modes of the GVIA−$Ca_V2.2$ complex are not predicted by ZDOCK even though two different structures of the toxin and channel are considered. Clearly, this is due to the artifacts of the rigid-body docking algorithm employed by ZDOCK. Although flexible docking algorithms such as HADDOCK[60] are available, their ability to handle molecular flexibility is generally very limited, and they are much less efficient than rigid-body algorithms computationally. To explore all the possible modes of binding of a toxin to a channel, multiple unbiased MD simulations may be performed.[17] Alternatively, biased MD simulation with distance restraints can be used. This is in analogy to the simulated annealing method used in determining molecular structures from NMR data. In biased MD, the flexibility of both the toxin and the channel is fully taken into account. In addition, appropriate distance restraints can be applied to steer the binding process rapidly, allowing any binding modes of interest to be examined with affordable computational cost. Therefore, biased MD presents an important alternative to molecular docking algorithms for the prediction of toxin−channel complex structures.

ω-Conotoxins are similar to μ-conotoxins, which are pore blockers of Na_V channels, and distinct from pore blocker toxins of K^+ channels primarily in two aspects. First, the conotoxins (20−30 residues) are typically smaller than K^+ channel blockers (35−40 residues). Second, both types of conotoxins are approximately globular in shape, whereas K^+ channel blockers are oval-shaped. The oval shape of K^+ channel blockers is important for maximizing the area of the toxin−channel interface and high-affinity binding. On the other hand, the globular shape of conotoxins and the approximately symmetrical distribution of basic residues would allow a conotoxin to inhibit its target channel with alternative binding modes, which should also enhance the ability of the toxin to block the channel.

Thus far, the only peptide toxin that has been shown to bind to a channel with multiple binding modes is μ-conotoxin PIIIA.[17] However, multiple binding modes have been demonstrated for several other protein−protein systems such as corticotropin releasing factor and its binding protein[61] and cohesin-dockerin.[62] In addition, it is well-known that various ligands can bind their receptor proteins in different modes.[63] In this work, we demonstrate that the Lys2 mode and the Arg17 mode are energetically equally favorable, indicating that GVIA inhibits $Ca_V2.2$ with multiple binding modes. We speculate that it may be common for globular ω-conotoxins to bind Ca_V channels with multiple alternative modes.

ASSOCIATED CONTENT

Supporting Information

Four figures showing two starting orientations of GVIA, structures of GVIA in complex with $Ca_V2.2$, and block analysis of the PMF profile for the Lys2 mode. This material is available free of charge via the Internet at http://pubs.acs.org.

AUTHOR INFORMATION

Corresponding Author

*E-mail: rong.chen@anu.edu.au. Phone: +61 2 6125 4337.

Funding

This work was supported by the National Health and Medical Research Council of Australia and The Medical Advances Without Animals Trust (MAWA).

Notes

The authors declare no competing financial interest.

ACKNOWLEDGMENTS

This research was undertaken on the NCI National Facility in Canberra, Australia, which is supported by the Australian Commonwealth Government.

ABBREVIATIONS

IC_{50}, half-maximal inhibition concentration; COM, center of mass; MD, molecular dynamics; PMF, potential of mean force.

REFERENCES

(1) Brennan, F., Carr, D. B., and Cousins, M. (2007) Pain management: A fundamental human right. *Anesth. Analg. (Hagerstown, MD, U.S.) 105*, 205−221.

(2) Catterall, W. A., Perez-Reyes, E., Snutch, T. P., and Striessnig, J. (2005) International Union of Pharmacology. XLVIII. Nomenclature and structure-function relationships of voltage-gated calcium channels. *Pharmacol. Rev. 57*, 411−425.

(3) Tanabe, T., Takeshima, H., Mikami, A., Flockerzi, V., Takahashi, H., Kangawa, K., Kojima, M., Matsuo, H., Hirose, T., and Numa, S. (1987) Primary structure of the receptor for calcium channel blockers from skeletal muscle. *Nature 328*, 313−318.

(4) Catterall, W. A. (2011) Voltage-gated calcium channels. *Cold Spring Harbor Perspect. Biol. 3*, a003947.

(5) Tranberg, C. E., Yang, A., Vetter, I., McArthur, J. R., Baell, J. B., Lewis, R. J., Tuck, K. L., and Duggan, P. J. (2012) ω-Conotoxin GVIA mimetics that bind and inhibit neuronal Cav2.2 ion channels. *Mar. Drugs 10*, 2349−2368.

(6) Saez, N. J., Senff, S., Jensen, J. E., Er, S. Y., Herzig, V., Rash, L. D., and King, G. F. (2010) Spider-venom peptides as therapeutics. *Toxins 2*, 2851−2871.

(7) Olivera, B. M., Cruz, L. J., Desantos, V., Lecheminant, G. W., Griffin, D., Zeikus, R., Mcintosh, J. M., Galyean, R., Varga, J., Gray, W. R., and Rivier, J. (1987) Neuronal calcium channel antagonists. Discrimination between calcium channel subtypes using ω-conotoxin from *Conus magus* venom. *Biochemistry 26*, 2086−2090.

(8) McGivern, J. G. (2007) Ziconotide: A review of its pharmacology and use in the treatment of pain. *Neuropsychiatr. Dis. Treat. 3*, 69−85.

(9) Kolosov, A., Aurini, L., Williams, E. D., Cooke, I., and Goodchild, C. S. (2011) Intravenous injection of leconotide, an omega conotoxin: Synergistic antihyperalgesic effects with morphine in a rat model of bone cancer pain. *Pain Med. 12*, 923−941.

(10) Witcher, D. R., De Waard, M., and Campbell, K. P. (1993) Characterization of the purified N-type Ca^{2+} channel and the cation

sensitivity of ω-conotoxin GVIA binding. *Neuropharmacology 32*, 1127−1139.
(11) Ellinor, P. T., Zhang, J. F., Horne, W. A., and Tsien, R. W. (1994) Structural determinants of the blockade of N-type calcium channels by a peptide neurotoxin. *Nature 372*, 272−275.
(12) McCleskey, E. W., Fox, A. P., Feldman, D. H., Cruz, L. J., Olivera, B. M., Tsien, R. W., and Yoshikami, D. (1987) ω-Conotoxin: Direct and persistent blockade of specific types of calcium channels in neurons but not muscle. *Proc. Natl. Acad. Sci. U.S.A. 84*, 4327−4331.
(13) Abe, T., Koyano, K., Saisu, H., Nishiuchi, Y., and Sakakibara, S. (1986) Binding of ω-conotoxin to receptor sites associated with the voltage-sensitive calcium channel. *Neurosci. Lett. 71*, 203−208.
(14) Nielsen, K. J., Schroeder, T., and Lewis, R. (2000) Structure-activity relationships of ω-conotoxins at N-type voltage-sensitive calcium channels. *J. Mol. Recognit. 13*, 55−70.
(15) Pallaghy, P. K., and Norton, R. S. (1999) Refined solution structure of ω-conotoxin GVIA: Implications for calcium channel binding. *J. Pept. Res. 53*, 343−351.
(16) Nielsen, K. J., Watson, M., Adams, D. J., Hammarstrom, A. K., Gage, P. W., Hill, J. M., Craik, D. J., Thomas, L., Adams, D., Alewood, P. F., and Lewis, R. J. (2002) Solution structure of μ-conotoxin PIIIA, a preferential inhibitor of persistent tetrodotoxin-sensitive sodium channels. *J. Biol. Chem. 277*, 27247−27255.
(17) Chen, R., and Chung, S. H. (2012) Binding modes of μ-conotoxin to the bacterial sodium channel (Na_VAb). *Biophys. J. 102*, 483−488.
(18) Finol-Urdaneta, R. K., Glavica, R., McArthur, J. R., and French, R. J. (2013) Polymodal, high affinity actions of μ-conotoxins on a bacterial voltage-gated sodium channel. *Biophys. J. 104*, 136a−137a.
(19) Jaravine, V. A., Nolde, D. E., Reibarkh, M. J., Korolkova, Y. V., Kozlov, S. A., Pluzhnikov, K. A., Grishin, E. V., and Arseniev, A. S. (1997) Three-dimensional structure of toxin OSK1 from *Orthochirus scrobiculosus* scorpion venom. *Biochemistry 36*, 1223−1232.
(20) Zhu, S., Peigneur, S., Gao, B., Luo, L., Jin, D., Zhao, Y., and Tytgat, J. (2011) Molecular diversity and functional evolution of scorpion potassium channel toxins. *Mol. Cell. Proteomics 10*, M110.002832.
(21) Chen, R., Robinson, A., Gordon, D., and Chung, S. H. (2011) Modeling the binding of three toxins to the voltage-gated potassium channel (Kv1.3). *Biophys. J. 101*, 2652−2660.
(22) Payandeh, J., Scheuer, T., Zheng, N., and Catterall, W. A. (2011) The crystal structure of a voltage-gated sodium channel. *Nature 475*, 353−358.
(23) McCusker, E. C., Bagneris, C., Naylor, C. E., Cole, A. R., D'Avanzo, N., Nichols, C. G., and Wallace, B. A. (2012) Structure of a bacterial voltage-gated sodium channel pore reveals mechanisms of opening and closing. *Nat. Commun. 3*, 1102.
(24) Payandeh, J., Gamal El-Din, T. M., Scheuer, T., Zheng, N., and Catterall, W. A. (2012) Crystal structure of a voltage-gated sodium channel in two potentially inactivated states. *Nature 486*, 135−139.
(25) Zhang, X., Ren, W., DeCaen, P., Yan, C., Tao, X., Tang, L., Wang, J., Hasegawa, K., Kumasaka, T., He, J., Wang, J., Clapham, D. E., and Yan, N. (2012) Crystal structure of an orthologue of the NaChBac voltage-gated sodium channel. *Nature 486*, 130−134.
(26) Dudley, S. C., Jr., Chang, N., Hall, J., Lipkind, G., Fozzard, H. A., and French, R. J. (2000) μ-Conotoxin GIIIA interactions with the voltage-gated Na^+ channel predict a clockwise arrangement of the domains. *J. Gen. Physiol. 116*, 679−690.
(27) Li, R. A., Ennis, I. L., French, R. J., Dudley, S. C., Jr., Tomaselli, G. F., and Marbán, E. (2001) Clockwise domain arrangement of the sodium channel revealed by μ-conotoxin (GIIIA) docking orientation. *J. Biol. Chem. 276*, 11072−11077.
(28) Mintseris, J., Pierce, B., Wiehe, K., Anderson, R., Chen, R., and Weng, Z. (2007) Integrating statistical pair potentials into protein complex prediction. *Proteins 69*, 511−520.
(29) Reynolds, I. J., Wagner, J. A., Snyder, S. H., Thayer, S. A., Olivera, B. M., and Miller, R. J. (1986) Brain voltage-sensitive calcium channel subtypes differentiated by ω-conotoxin fraction GVIA. *Proc. Natl. Acad. Sci. U.S.A. 83*, 8804−8807.
(30) Eriksson, M. A., and Roux, B. (2002) Modeling the structure of agitoxin in complex with the *Shaker* K^+ channel: A computational approach based on experimental distance restraints extracted from thermodynamic mutant cycles. *Biophys. J. 83*, 2595−2609.
(31) Chen, R., and Chung, S. H. (2012) Structural basis of the selective block of Kv1.2 by maurotoxin from computer simulations. *PLoS One 7*, e47253.
(32) Phillips, J. C., Braun, R., Wang, W., Gumbart, J., Tajkhorshid, E., Villa, E., Chipot, C., Skeel, R. D., Kalé, L., and Schulten, K. (2005) Scalable molecular dynamics with NAMD. *J. Comput. Chem. 26*, 1781−1802.
(33) MacKerell, A. D., Bashford, D., Bellott, M., Dunbrack, R. L., Evanseck, J. D., Field, M. J., Fischer, S., Gao, J., Guo, H., Ha, S., Joseph-McCarthy, D., Kuchnir, L., Kuczera, K., Lau, F. T. K., Mattos, C., Michnick, S., Ngo, T., Nguyen, D. T., Prodhom, B., Reiher, W. E., Roux, B., Schlenkrich, M., Smith, J. C., Stote, R., Straub, J., Watanabe, M., Wiórkiewicz-Kuczera, J., Yin, D., and Karplus, M. (1998) All-atom empirical potential for molecular modeling and dynamics studies of proteins. *J. Phys. Chem. B 102*, 3586−3616.
(34) Klauda, J. B., Venable, R. M., Freites, J. A., O'Connor, J. W., Tobias, D. J., Mondragon-Ramirez, C., Vorobyov, I., MacKerell, A. D., Jr., and Pastor, R. W. (2010) Update of the CHARMM all-atom additive force field for lipids: Validation on six lipid types. *J. Phys. Chem. B 114*, 7830−7843.
(35) Jorgensen, W. L., Chandrasekhar, J., Madura, J. D., Impey, R. W., and Klein, M. L. (1982) Comparison of simple potential functions for simulating liquid water. *J. Chem. Phys. 79*, 926−935.
(36) Ryckaert, J. P., Ciccotti, G., and Berendsen, H. J. C. (1977) Numerical integration of the cartesian equations of motion of a system with constraints: Molecular dynamics of *n*-alkanes. *J. Comput. Phys. 23*, 327−341.
(37) Miyamoto, S., and Kollman, P. A. (1992) SETTLE: An analytical version of the SHAKE and RATTLE algorithm for rigid water models. *J. Comput. Chem. 13*, 952−962.
(38) Humphrey, W., Dalke, A., and Schulten, K. (1996) VMD: Visual molecular dynamics. *J. Mol. Graphics 14*, 33−38.
(39) Allen, T. W., Andersen, O. S., and Roux, B. (2004) Energetics of ion conduction through the gramicidin channel. *Proc. Natl. Acad. Sci. U.S.A. 101*, 117−122.
(40) Gordon, D., Chen, R., and Chung, S. H. (2013) Computational methods of studying the binding of toxins from venomous animals to biological ion channels: Theory and applications. *Physiol. Rev. 93*, 767−802.
(41) Kumar, S., and Nussinov, R. (2002) Close-range electrostatic interactions in proteins. *ChemBioChem 3*, 604−617.
(42) Mills, J. E., and Dean, P. M. (1996) Three-dimensional hydrogen-bond geometry and probability information from a crystal survey. *J. Comput.-Aided Mol. Des. 10*, 607−622.
(43) Kumar, S., Bouzida, D., Swendsen, R. H., Kollman, P. A., and Rosenberg, J. M. (1992) The weighted histogram analysis method for free-energy calculations on biomolecules. I. The method. *J. Comput. Chem. 13*, 1011−1021.
(44) Lew, M. J., Flinn, J. P., Pallaghy, P. K., Murphy, R., Whorlow, S. L., Wright, C. E., Norton, R. S., and Angus, J. A. (1997) Structure-function relationships of ω-conotoxin GVIA. Synthesis, structure, calcium channel binding, and functional assay of alanine-substituted analogues. *J. Biol. Chem. 272*, 12014−12023.
(45) Flinn, J. P., Pallaghy, P. K., Lew, M. J., Murphy, R., Angus, J. A., and Norton, R. S. (1999) Roles of key functional groups in ω-conotoxin GVIA. Synthesis, structure and functional assay of selected peptide analogues. *Eur. J. Biochem. 262*, 447−455.
(46) Kim, J. I., Takahashi, M., Ogura, A., Kohno, T., Kudo, Y., and Sato, K. (1994) Hydroxyl group of Tyr^{13} is essential for the activity of ω-conotoxin GVIA, a peptide toxin for N-type calcium channel. *J. Biol. Chem. 269*, 23876−23878.
(47) Carnevale, V., Treptow, W., and Klein, M. L. (2011) Sodium ion binding sites and hydration in the lumen of a bacterial ion channel from molecular dynamics simulations. *J. Phys. Chem. Lett. 2*, 2504−2508.

(48) Wagner, J. A., Snowman, A. M., Biswas, A., Olivera, B. M., and Snyder, S. H. (1988) ω-Conotoxin GVIA binding to a high-affinity receptor in brain: Characterization, calcium sensitivity, and solubilization. *J. Neurosci. 8*, 3354−3359.
(49) Lewis, R. J., Nielsen, K. J., Craik, D. J., Loughnan, M. L., Adams, D. A., Sharpe, I. A., Luchian, T., Adams, D. J., Bond, T., Thomas, L., Jones, A., Matheson, J. L., Drinkwater, R., Andrews, P. R., and Alewood, P. F. (2000) Novel ω-conotoxins from *Conus catus* discriminate among neuronal calcium channel subtypes. *J. Biol. Chem. 275*, 35335−35344.
(50) Wimley, W. C., Gawrisch, K., Creamer, T. P., and White, S. H. (1996) Direct measurement of salt-bridge solvation energies using a peptide model system: Implications for protein stability. *Proc. Natl. Acad. Sci. U.S.A. 93*, 2985−2990.
(51) Anderson, D. E., Becktel, W. J., and Dahlquist, F. W. (1990) pH-induced denaturation of proteins: A single salt bridge contributes 3−5 kcal/mol to the free energy of folding of T4 lysozyme. *Biochemistry 29*, 2403−2408.
(52) Aiyar, J., Withka, J. M., Rizzi, J. P., Singleton, D. H., Andrews, G. C., Lin, W., Boyd, J., Hanson, D. C., Simon, M., Dethlefs, B., Lee, C., Hall, J. E., Gutman, G. A., and Chandy, K. G. (1995) Topology of the pore-region of a K^+ channel revealed by the NMR-derived structures of scorpion toxins. *Neuron 15*, 1169−1181.
(53) Sheu, S. Y., Yang, D. Y., Selzle, H. L., and Schlag, E. W. (2003) Energetics of hydrogen bonds in peptides. *Proc. Natl. Acad. Sci. U.S.A. 100*, 12683−12687.
(54) Williams, D. H., Searle, M. S., Mackay, J. P., Gerhard, U., and Maplestone, R. A. (1993) Toward an estimation of binding constants in aqueous solution: Studies of associations of vancomycin group antibiotics. *Proc. Natl. Acad. Sci. U.S.A. 90*, 1172−1178.
(55) Jin, L., and Wu, Y. (2011) Molecular mechanism of δ-dendrotoxin-potassium channel recognition explored by docking and molecular dynamic simulations. *J. Mol. Recognit. 24*, 101−107.
(56) Yi, H., Qiu, S., Wu, Y., Li, W. X., and Wang, B. (2011) Differential molecular information of maurotoxin peptide recognizing IK_{Ca} and Kv1.2 channels explored by computational simulation. *BMC Struct. Biol. 11*, 3.
(57) Chen, R., Robinson, A., and Chung, S. H. (2012) Binding of hanatoxin to the voltage sensor of Kv2.1. *Toxins 4*, 1552−1564.
(58) Khabiri, M., Nikouee, A., Cwiklik, L., Grissmer, S., and Ettrich, R. (2011) Charybdotoxin unbinding from the mKv1.3 potassium channel: A combined computational and experimental study. *J. Phys. Chem. B 115*, 11490−11500.
(59) Chen, P. C., and Kuyucak, S. (2012) Developing a comparative docking protocol for the prediction of peptide selectivity profiles: Investigation of potassium channel toxins. *Toxins 4*, 110−138.
(60) Dominguez, C., Boelens, R., and Bonvin, A. M. (2003) HADDOCK: A protein-protein docking approach based on biochemical or biophysical information. *J. Am. Chem. Soc. 125*, 1731−1737.
(61) Potter, E., Behan, D. P., Linton, E. A., Lowry, P. J., Sawchenko, P. E., and Vale, W. W. (1992) The central distribution of a corticotropin-releasing factor (CRF)-binding protein predicts multiple sites and modes of interaction with CRF. *Proc. Natl. Acad. Sci. U.S.A. 89*, 4192−4196.
(62) Carvalho, A. L., Dias, F. M., Nagy, T., Prates, J. A., Proctor, M. R., Smith, N., Bayer, E. A., Davies, G. J., Ferreira, L. M., Romao, M. J., Fontes, C. M., and Gilbert, H. J. (2007) Evidence for a dual binding mode of dockerin modules to cohesins. *Proc. Natl. Acad. Sci. U.S.A. 104*, 3089−3094.
(63) Lewi, P. J., de Jonge, M., Daeyaert, F., Koymans, L., Vinkers, M., Heeres, J., Janssen, P. A., Arnold, E., Das, K., Clark, A. D., Jr., Hughes, S. H., Boyer, P. L., deBethune, M. P., Pauwels, R., Andries, K., Kukla, M., Ludovici, D., DeCorte, B., Kavash, R., and Ho, C. (2003) On the detection of multiple-binding modes of ligands to proteins, from biological, structural, and modeling data. *J. Comput.-Aided Mol. Des. 17*, 129−134.